Effect of Mechanical Activation on Ti_3AlC_2 Max Phase Formation under Self-Propagating High-Temperature Synthesis

A.Yu. Potanin[1*], P.A. Loginov[1], E.A. Levashov[1], Yu.S. Pogozhev[1], E.I. Patsera[1], N.A. Kochetov[2]

[1]National University of Science and Technology "MISIS", SHS Research & Education Center MISIS-ISMAN, Leninsky prospect, 4, Moscow, 119049, Russia
[2]Institute of Structural Macrokinetics and Materials Science, Russian Academy of Sciences, ul. Academica Osipyana, 8, Chernogolovka, Moscow Region, 142432 Russia

Article info

Received:
9 March 2014

Received and revised form:
27 April 2015

Accepted:
5 June 2015

Keywords:
SHS, mechanical activation, mechanosynthesis, Ti_3AlC_2, combustion rate

Abstract

In this study, we have investigated the effect of various mechanical activation (MA) modes on phase and structure formation in powder mixtures made up to produce Ti_3AlC_2 MAX phase. The optimal MA duration has been established which results in the maximum heat release under SHS due to accumulation of structural defects leading to the growth of internal energy. The effect of MA on the character and kinetics of combustion front propagation has been investigated. It was shown that following pretreatment of a powder mixture in a planetary ball mill, the combustion mode changes from stationary to a pulsating combustion and, consequently, the combustion rate decreases. The burning-out of the sample is partial and with interruptions (depressions). Force SHS-pressing technology was used for obtaining of compacted samples with homogeneous structure based on Ti_3AlC_2.

1. Introduction

MAX phases ($M_{n+1}AX_n$, where M is a transition metal, A is, predominantly, a IIIA or IVA element, and X is either carbon or nitrogen) are high-melting non-oxide compounds with a hexagonal layered structure and unique combination of metal and ceramic properties [1]. Like metals, they are thermally and electrically conductive, readily machinable at room temperature, resistant to crack propagation and thermal shock, and they deform plastically at elevated temperatures. Like ceramics, they have low density, high elastic modulus, excellent heat resistance and high temperature strength [2]. Due to their layered structure and similarly to hexagonal boron nitride and graphite, these materials are easily machinable [3]. The combination of all these properties make materials based on MAX phases quite suitable for many high-temperature structural and functional applications.

Most studies in Ti–Al–C system consider MAX phases of Ti_2AlC and Ti_3AlC_2 compounds [4]. Ti_2AlC has the highest melting point (1625 °C) and it is stable at high temperatures, however, if the temperature decreases lower than 1500 °C, the compound decomposes and goes over to Ti_3AlC_2 MAX phase via the following reaction: $2Ti_2AlC \rightarrow Ti_3AlC_2 + TiAl_{1-x} + xAl_{(gas)}$ [5]. Ti_3AlC_2 has better thermal stability, higher elasticity modulus and hardness as compared to Ti_2AlC. Moreover, Ti_3AlC_2 is ductile under compression [6].

Ti_3AlC_2 was first synthesized by sintering of Ti, TiAl, Al_4C_3 and C compacted powder mixtures at the temperature of 1300 °C for 20 h in the reducing atmosphere (H_2) [7]. Further investigations explored both variations in the chemical and phase compositions of the reaction mixtures [1, 8–10] and application of various synthesis methods: hot isostatic pressing, hot pressing and spark plasma sintering [11–13].

In addition to the aforementioned conventional methods used to synthesize this compound, self-propagating high-temperature synthesis (SHS) has also been studied [14–16]. This method uses chemical energy (combustion mode) released in the process of exothermic reactions between the initial powder components.

One of the areas of application of the materials based on MAX phases and synthesized by SHS is producing multicomponent sputtered targets (cath-

* Corresponding author. E-mail: a.potanin@inbox.ru

odes) and electrodes for the application of multifunctional coatings using a magnetron technique and pulsed electro-spark deposition. The obtained coatings have excellent physical, mechanical and service properties [17, 18].

Depending on the synthesis method, the formation mechanism of Ti_3AlC_2 MAX phase can be divided into two groups:

1) Methods using slow heating of initial components [1, 11, 19, 20]. The formation mechanism of MAX phase is as follows: aluminum is melted at the temperature of 660 °C and, spreading over titanium and carbon black particles, it produces the reaction surface with the formation of $TiAl_3$ or $TiAl_2$ intermediate compounds. Further, as this reaction develops, diffusion saturation of $TiAl_x$ with titanium occurs and TiAl and Ti_3Al are produced. At the second stage, titanium carbide is produced which enters into a reaction with intermetallides or aluminium melt, with the formation of ternary compounds:

$$TiC_x + Ti_xAl_y \rightarrow Ti_{x+1}AlC_x$$

$$TiC_x + Al \rightarrow Ti_{x+1}AlC_x$$

2) In case of SHS [3, 10, 14–16], the formation mechanism of $Ti_{x+1}AlC_x$ compounds is slightly different to the one described above. This is caused by higher combustion rate and temperature values. Both aluminum and titanium are melted in the combustion wave, and reaction surface is formed by the titanium-aluminum melt spreading over the carbon black surface. As far as this melt is being saturated with carbon, titanium carbide grains are precipitating. $M_{n+1}AX_n$ phases in Ti–Al–C system are formed at the stage of the secondary structure formation through the interaction of TiC_x Ti–Al melt.

It is known that in order to increase the rate of conversion, structural and phase homogeneity of combustion products and, consequently, enhance the content of various ternary compounds including MAX phases; the reactive mixture is subjected to preliminary mechanical activation (MA) [21–24]. Due to severe plastic deformation processes, MA results in the significant reduction of mixture heterogeneity and accumulation of energy at the reactant structure defects [25–27]. Therefore, MA of the reactive mixture can increase the combustion rate, reduce the temperature at which the reaction occurs, as well as ignition temperature due to the enhanced total reaction surface [28, 29]. However, the mentioned studies also reveal that long-term intense mechanical impact in the mill jars leads to the occurrence of mechanochemical reactions and formation of interaction products. This results in a lower combustion rate and temperature.

This work was aimed at studying the effect of mechanical activation on structural and phase transitions in 3Ti + Al + 2C powder mixture, character and kinetics of combustion front propagation, and structure of SHS ceramics based on Ti_3AlC_2.

1.1. Materials and experimental techniques

PTS titanium (TU 14-22-57-92), ASD-1 aluminum and P804T carbon black powders were used as initial components of the reactive mixture. The reactants with the molar ratio of 3: 1: 2 (based on the formation of Ti_3AlC_2) were mixed in a ball mill (BM) with the use of steel grinding media for 16 hours. The powder to ball ratio was 1:8. The mixture was mechanically activated in the Activator-2S high-speed centrifugal planetary mill (CPM) in Ar inert atmosphere (1 atm.), with the operating parameters being as follows: jar volume – 250 cm^3, rotation rate – 900 rpm (120 g), powder to ball ratio 1:15. Due to partial Al evaporation at high temperatures and losses resulting from powder rubbing against the walls and balls of the mixing jar and in order to improve the stoichiometry, Al powder was added in excess of 2 wt.%.

Heat release and its rate in the combustion reaction were determined using a BKS-2H fast combustion calorimeter accurate up to 0.2% in the range of $10^3 – 10^4$ J.

The combustion temperature and rate were measured in a laboratory SHS reactor. Pellets of 10 mm in diameter and 20 mm in height with the relative density of 55% were produced from the raw mixture by double-side pressing. W-Re 5/20 thermocouple installed inside the pellet in a hole with the depth of ~5 mm was used to determine the combustion temperature. The combustion rate was measured by high-speed video recording using a Panasonic WV-BL600 camera with a laboratory-size lens at 15-fold magnification.

The phase composition of combustion products was examined by X-ray diffraction analysis (XRD). The spectra were processed using the JCPDS database and designated software package developed at National University of Science and Technology MISiS. The microstructure was examined using a Hitachi S-3400N scanning electronic microscope (Japan). The fine structure of powder samples was studied by transmission electron microscopy (TEM) using a JEM-2100 device equipped with an Oxford INCA energy-dispersive X-ray spectrometer.

IR spectroscopy measurements were carried out in an attenuated total reflectance (ATR) mode using a Vertex 70v vacuum spectrometer (Bruker) in the range of 500–4000 cm^{-1} with a resolution of 4 cm^{-1}.

All IR spectra were treated by baseline correction.

Compacted samples were synthesized by force SHS-pressing technology. A pellet made of raw mixture of 48 mm in diameter compacted to the relative density of 55–60% was synthesized in a sand reaction mold on a DA-1532B hydraulic press. After the process has been completed, hot synthesized products were pressed at the pressure of 7 MPa. As soon as the process of force SHS-pressing was finished, the mold was discharged. Then the hot synthesized products underwent thermal treatment in a muffle furnace in air atmosphere at the temperature of 1100 °C for 30 min. The obtained materials were further cooled together with the furnace down to the room temperature

2. Results and Discussion

In order to assess the effect of MA on the reactive capacity of the mixture, the morphology and structural condition of Ti–Al–C powder mixtures subjected to MA for 1–5 min were investigated. The coherent scattering region sizes (CSR) and microstrain (ε) of the Ti and Al lattice were determined using X-ray diffraction analysis. Figure 1 shows XDR patterns, and Table 1 provides the explanation. We can see that MA for 1–4 min results in the reduced sizes of coherent scattering regions and bigger ε value. This indicates the accumulation of defects in the crystalline structure of the material and increase of the stored energy. The mixture prepared in a BM contains TiH_2 in addition to α-Ti and Al phases (C was in the amorphous state.) Titanium hydride is present in the powder mixture due to the calcium hydride method used to produce Ti powder. According to TU 14-22-57-92, this amount of hydrogen is acceptable. By adding TiH_2, the content of Ti_3AlC_2 MAX phase can be increased after SHS [16].

MA for 1–2 min has no effect on the phase composition of the mixture. And severe plastic deformation results only in crystallite refining which is proved by broadening of the peaks corresponding to α-Ti and Al phases.

The XRD pattern of the powder mixture exposed to MA for 3 min shows the lines of TiC phase. If MA duration is increased up to 4 min, Ti_3AlC_2 phase is formed. After being exposed to MA for 5 min, the mixture is practically free of the initial reactants. This powder contains Ti_3AlC_2 (45%), TiC (34%) and Ti_2AlC (13%). The presence of the latter two phases most probably indicates the lack of Al, which is deposited on the surface of grinding media and jar walls after the treatment.

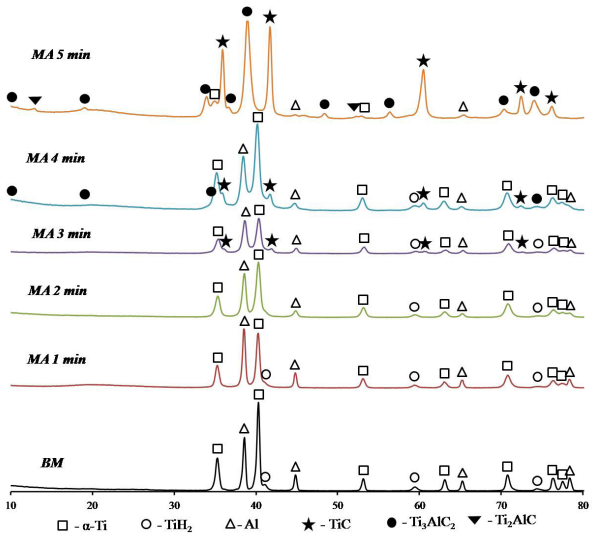

Fig. 1. XRD patterns of 3Ti + Al + 2C powder mixtures prepared in a BM and exposed to MA for 1–5 min.

Table 1

Effect of mechanical activation (MA) duration on the phase composition of the mixture, size of coherent scattering regions and microstrain of the Ti and Al lattice.

Phase	α-Ti (*hP*2/1)			Al (*cF*4/1)			TiH_2 (*cF*12/1)	TiC (*cF*8/2)	Ti_3AlC_2 (*hP*12/7)	Ti_2AlC (*hP*8/4)
Duration of MA, min	wt.%	CSR size, Å	ε, %	wt.%	CSR size, Å	ε, %	wt.%	wt.%	wt.%	wt.%
1	64	470 ± 50	0.22 ± 0.02	25	~ 3000	0.09 ± 0.01	11	-	-	-
2	75	299 ± 30	0.23 ±0.02	15	298 ± 30	0.10 ± 0.01	10	-	-	-
3	63	246 ± 30	025 ± 0.03	19	283 ± 30	0.11 ± 0.01	10	8	-	-
4	60	217 ± 25	0.25 ± 0.01	13	194 ± 22	0.14 ± 0.01	10	11	6	-
5	-			3	-		5	34	45	13

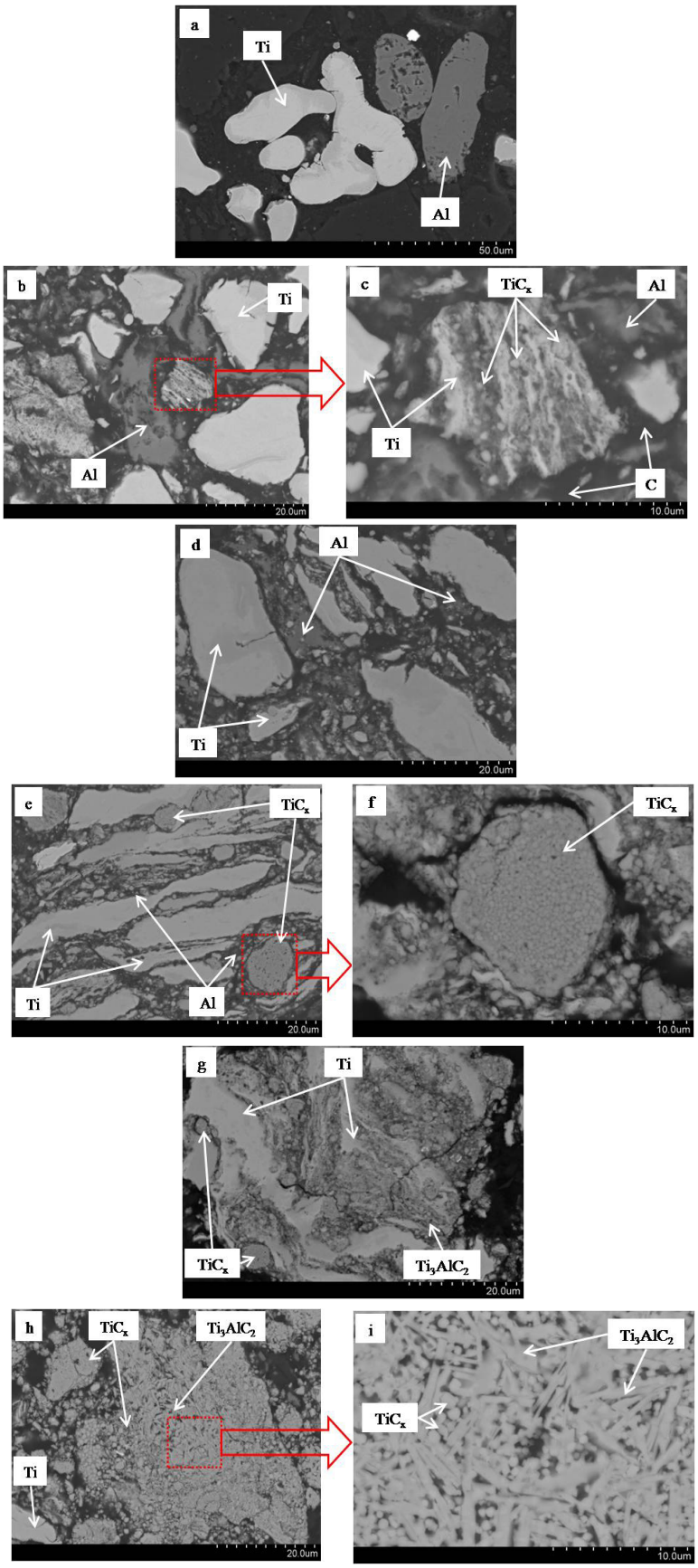

Fig. 2. Evolution of microstructure of 3Ti + Al + 2C powder mixtures prepared in a BM (a) and exposed to MA for 1 (b, c), 2 (d), 3 (e, f), 4 (g) and 5 (h, i) min.

Figure 2 presents the microstructure of 3Ti + Al + 2C mixtures treated in a BM and CPM for various time periods. The particles of Ti powder are represented as light gray areas, Al particles are shown as dark gray area, and fine C particles are in the black filling of carbon-containing resin section and, therefore, they are not observable by back-scattered electron (BSE) diffraction. The treatment of a mixture in a BM ensures the initial components are mixed practically without changing their form and sizes (Fig. 2a). MA for 1 min results in the increased average size of the mixture particles caused by grain formation under plastic deformation. Al particles are deformed, the carbon black is refined to a submicron state and covers Ti particles (Fig. 2b). Due to collision with the grinding media, C diffuses into Ti grains and enters into a reaction with TiC producing [30] (Fig. 2c). The content of TiC phase is too low to be detected by XRD. In order to prove its presence, the powder mixture was examined using TEM (×25000–50000) with energy-dispersive X-ray spectroscopy (EDX) (Fig. 3). It was demonstrated that the chemical composition of the circular grains 0.7–1.0 μm in size corresponded to that of nonstoichiometric titanium carbide TiC_x. In addition to structural determinations, the mixtures exposed to MA (1–5 min) were analyzed using IR spectroscopy. For the purposes of comparison, the spectra of TiC pure powder were recorded (Fig. 4.) We can see that the peak at 500 cm^{-1} characteristic of Ti–C [31] is present in the spectra of all mixtures, including those exposed to MA for 1 min. This fact indicates that the components begin to react with each other in CPM jars.

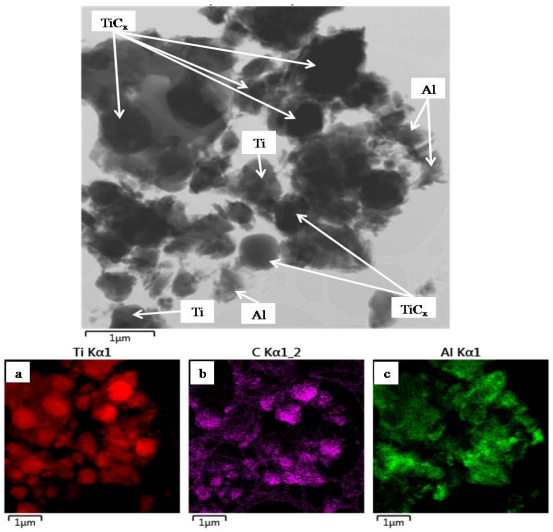

Fig. 3. Maps of element distribution in 3Ti + Al + 2C powder exposed to MA for 1 min. Imaging using characteristic radiation of Ti (a), C (b) and Al (c).

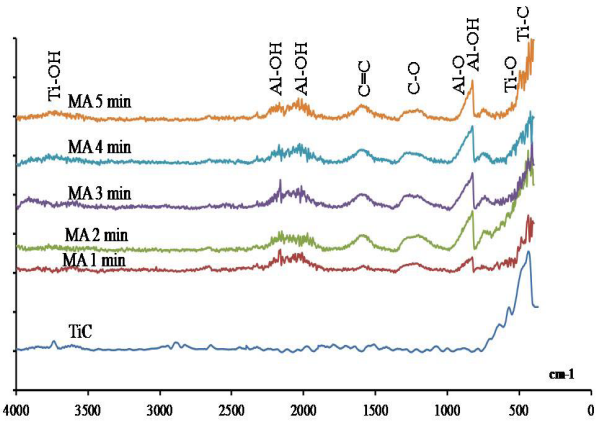

Fig. 4. IR spectra of mechanically activated 3Ti + Al +2C mixtures and TiC powder.

The longer duration of MA leads to further deformation of Ti and Al particles and formation of reaction products in the mixture (Fig. 2d). The mixture components exposed to MA for 3 min form layered composite granules with an extended contact (reaction) surface (Fig. 2e), where Ti and Al form alternating layers 1–10 μm in thickness. Normally, these layers are parallel. Note also a significant increase in the contents of titanium carbide represented as large polycrystalline particles (Fig. 2f).

After exposure to MA for 4 min, the average thickness of Ti and Al layers is reduced (Fig. 2g). Only large Ti grains are clearly noticeable in the structure of powder grains, the amount of TiC_x grains is increased. The presence of Ti_3AlC_2 phase detected by XRD was also confirmed using TEM and EDS methods (Fig. 5). Particle with a composition similar to Ti_3AlC_2 were discovered on the distribution maps of elements produced from this powder. The lattice type (hexagonal) and lattice spacing values determined using the XRD pattern recorded for these particles (at the areas 150 nm in size) corresponded to Ti_3AlC_2 phase (see the insert in Fig. 5.) Afterwards, by the 5th min of MA, Ti_3AlC_2 and TiC are completely synthesized in the jars. Figures 2h and 2i demonstrate that powder particles include only the grains of phases that are products of MA.

Using the technique described in the referenced study [32], experimental dependences of heat release value (Q) and heat release rate (Φ) during the combustion on the duration of MA were plotted (Fig. 6). We can see that both values increase with longer duration of MA. This is caused by the increased rate of conversion in the combustion reaction resulting from the accumulation of micro- and macrodefects in the initial powders, which leads to the growth of internal energy and reduced mixture heterogeneity

[25–27]. The optimal duration of MA that ensures the maximum heat release of the raw mixture is 3 min. If the activation time is further increased, the heat release becomes lower as the amount of reactants is reduced due to the partial formation of synthesized products in the mill jar. The inert components are accumulated, and heat losses associated with their heating and melting are increased.

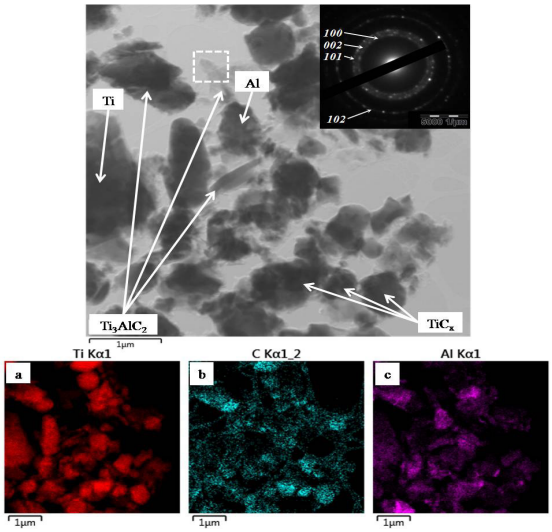

Fig. 5. Maps of element distribution in 3Ti + Al + 2C powder exposed to MA for 4 min. Imaging using characteristic radiation of Ti (a), C (b) and Al (c).

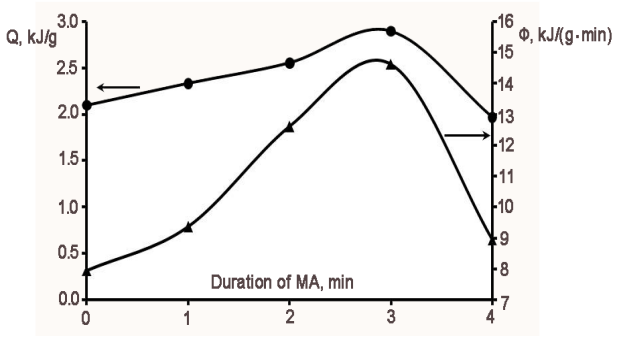

Fig. 6. Dependence of the amount of heat release (Q) and heat release rate (Φ) on the duration of mechanical activation.

Structural variations in the reactive mixture caused by MA have a significant effect on the character of combustion wave propagation. It was observed that the raw mixture prepared in a BM is characterized by a conventional stationary combustion mode where all the points in a combustion wave move at a constant rate. However, it was quite unexpected to discover that the combustion front propagated in non-steady (pulsating) mode in all mechanically activated mixtures regardless of the duration of MA in the interval of 1–4 min (the mixture was not initiated, if MA continued for 5 min). Therefore, a detailed analysis of the character of combustion front propagation was required. It is shown that the pulsating mode is related to the formation of slip cracks resulting from gas release in the pellet made of raw mixture in the heating zone ahead of the combustion front. Following the gas release, both the actual heat conductivity in a heterogeneous medium and combustion rate are reduced. The results of IR spectroscopy (Fig. 4) demonstrate that activated compositions contain the bonds of hydroxylic and oxide Ti-OH, Al-OH, C-O groups. This indicates the presence of easily decomposable chemical compounds and adsorbed gases in the powders. The reduction of the combustion rate in the mixtures exposed to MA resulting from the transition to a non-steady combustion mode was also mentioned before [33].

The combustion had similar character in all mechanically activated mixtures. The sample decomposed to several parts (pieces). Figure 7 presents video shots of the combustion of a mixture treated in the BM (Fig. 7a) and mixture exposed to MA for 1 min (Fig. 7b). Pulses of the SHS front and escaping sparks (Fig. 7b) prove the assumption on the reduction of the average combustion rate caused by the intense gas release and change of the combustion mode.

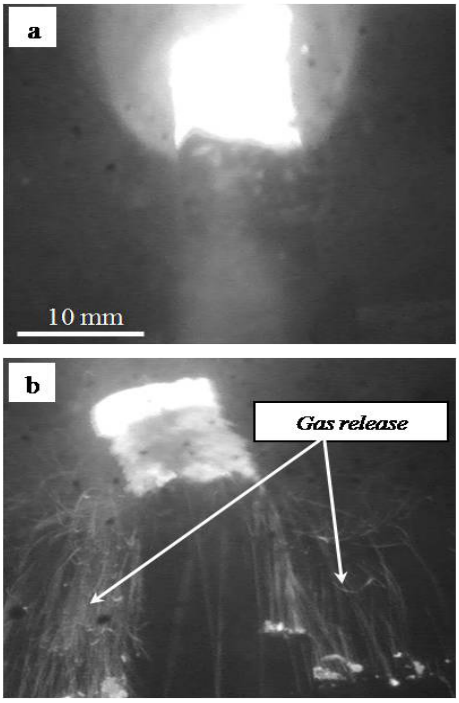

Fig. 7. Video shots of the combustion wave in 3Ti + Al + 2C mixture prepared in the BM (a) and exposed to mechanical activation for 1 min (b).

Since it is difficult to observe the effect of MA based on the average value of the combustion rate in a pulsating mode, the authors attempted to measure the local linear combustion rate at the flash and front stop periods (0.08–0.32 s.) Thus, the peak values of the combustion rate and pulse frequency were determined at several congruent segments (Fig. 8). We can see that if the duration of MA is increased from 1 to 3 min, the pulsation amplitude goes up from 6–7 mm/s to 12–14 mm/s, and if the duration of MA is increased to 4 min, the peak value of the combustion rate is reduced down to 7 mm/s. This is consistent with the results of fast combustion calorimetry (Fig. 6) showing that the accumulation of reaction products in the raw mixture occurs after the 3rd min. Figure 8 demonstrates that pulse frequency (self-oscillations) is reduced with the increased duration of MA.

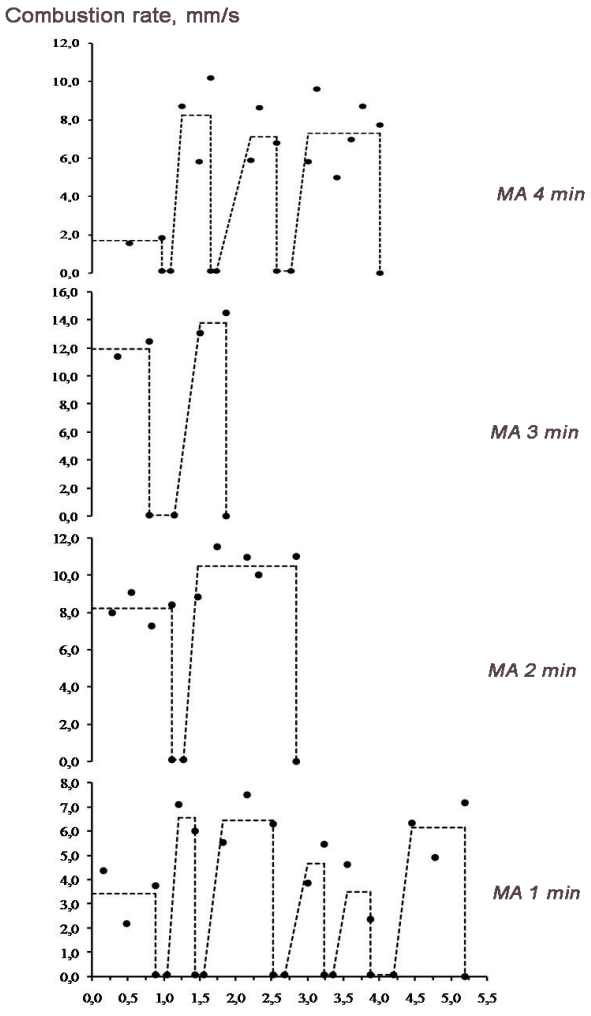

Fig. 8. Change of the local combustion rate of MA mixtures in the pulsating mode.

The mixture, which has been activated for 4 min, demonstrated the maximum spread of combustion rate values. This is probably related to the highest contents of the finished product in its composition, which restricts the reaction surface and impedes combustion.

Figure 9 presents the curve showing the dependence of the front coordinate and local combustion on time for the raw mixture after the 4th min of MA. Horizontal sections correspond to the depression period, and inclined sections comply with the period of active SHS front propagation. We can see that the more inclined lines of combustion front propagation correspond to higher values of the combustion rate.

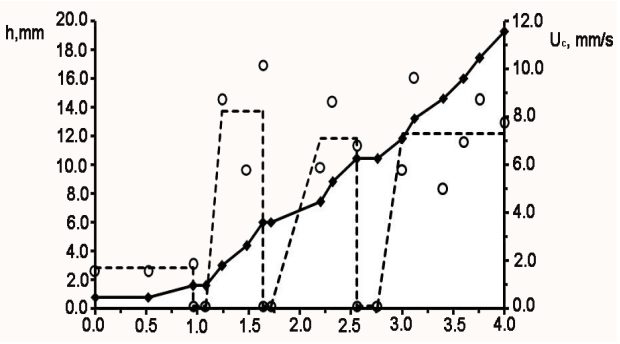

Fig. 9. Dependence of the front coordinate (continuous line) and averaged local combustion rate in the pulsating mode (dotted line) on time.

Figure 10 shows the dependence of combustion temperature and peak value of the local combustion rate in MA mixtures (measurements were taken in all areas and then averaged). The combustion rate value for the sample of the BM mixture is also plotted on the graph. A gradual decrease in the combustion with longer duration of MA is associated with the accumulation of TiC_x reaction product in the mixture, and MAX phases in Ti–Al–C system are formed at the stage of the secondary structure formation [34].

The following dependence was observed for the local combustion rate. First, the values go down with the transition from the stationary to pulsating mode. When the duration of MA is from 1 to 3 min, the rate increases due to the accumulation of energy at the structure defects and enhancement of the reactant specific surface area during the formation of composite granules with a layered structure. When the duration of MA is increased to 4 min, the combustion rate goes down.

Therefore, the mechanical activation of 3Ti + Al + 2C reactive mixture is accompanied by competing processes as follows: on the one hand, the enhance-

ment of the reactant surface and accumulation of energy at the structure defects, on the other hand, partial chemical conversion restricting the energy capacity of the system. When the duration of MA is up to 3 min, the first factor prevails. However, the second factor becomes predominant after the third minute of MA. The example when depending on MA parameters the predominant factor changes was previously investigated in detail and described using a mathematical model [35].

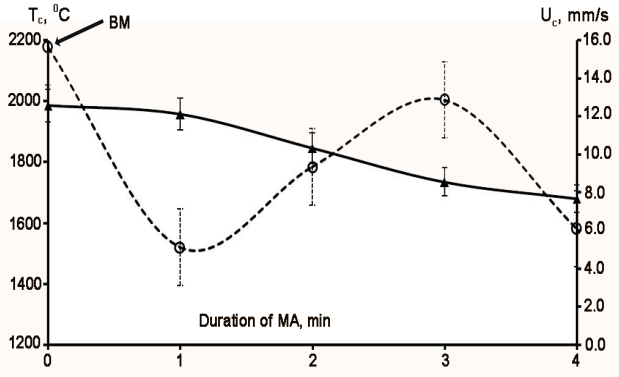

Fig. 10. Experimental values of the temperature (full line) and rate (dots) depending on the duration of MA.

Compacted ceramic materials were produced using force SHS-pressing technology. Mixtures of two types were used for synthesis: prepared in a BM and activated for 3 min. X-ray diffraction patterns and phase composition of the obtained samples are shown in Fig. 11. We can see that the sample obtained from MA mixture has higher rate of conversion and, consequently, higher content of Ti_3AlC_2 MAX phase. The observed lattice spacing values for Ti_3AlC_2 in MA sample are closer to tabular data a = 3.069 Å, c = 18.501 Å (ICDD Card No. 52-0875.) The products also contain nonstoichiometric titanium carbide with the target values of lattice spacing 4.324 Å and 4.320 Å, which corresponds to $TiC_{0.78}$ (for the BM sample) and $TiC_{0.7}$ (for the MA sample) [36]. Titanium carbide is always present as an intermediate phase in the synthesis of MAX phases [1, 3, 10, 14–16, 21–23]. The presence of this phase in the synthesized products is probably related to the incomplete chemical interaction of titanium carbide with the melt within the process cycle.

Figure 12 shows the fracture microstructure of the material synthesized from MA mixture. The synthesized product has composite two-phase structure which consists of Ti_3AlC_2 MAX phase with a layered (terraced) structure and circular TiC grains with particles 3 μm in size. Similar structural characteristics of the synthesized products in Ti–Al–C system were observed in previous studies [1, 3, 10, 14–16, 21–23]. After more detailed investigation of the melt microstructure, Ti_3AlC_2 grains were found to consist of a few superimposed layers, being approximately 0.5 μm in thickness.

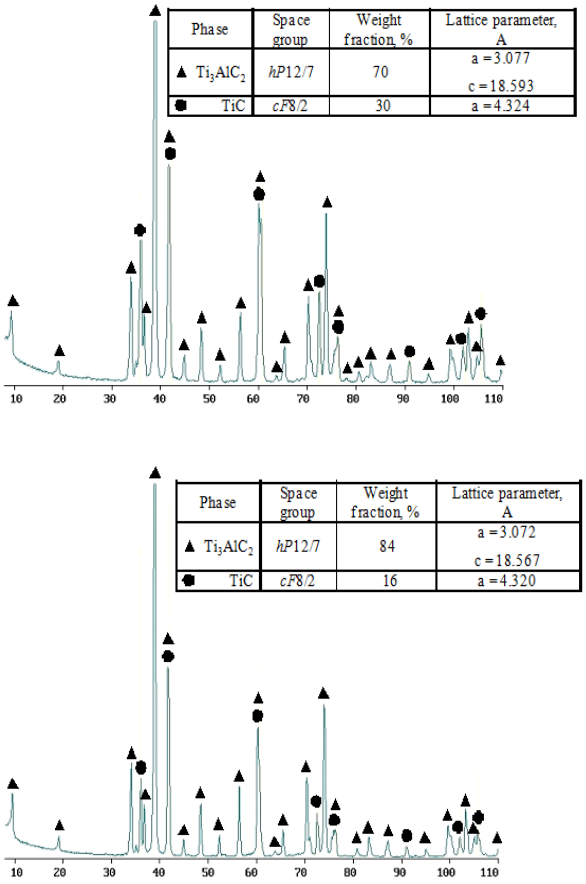

Fig. 11. XRD patterns of the material synthesized from non-activated (a) and activated (b) raw mixtures.

3. Conclusions

1. The effect of mechanical activation on structural and phase transitions in 3Ti + Al + 2C powder mixture has been investigated. It was demonstrated that the mechanical activation results in the structural variations as follows: deformation of the initial components, formation of layered composite granules, reduced coherent scattering region sizes, formation of mechanical synthesis products (TiC_x, Ti_3AlC_2).

2. Despite the product formation within the first period of activation, the amount of heat released in the reaction and heat release rate are increased. The optimal duration of MA in terms of the maximum heat release is 3 min.

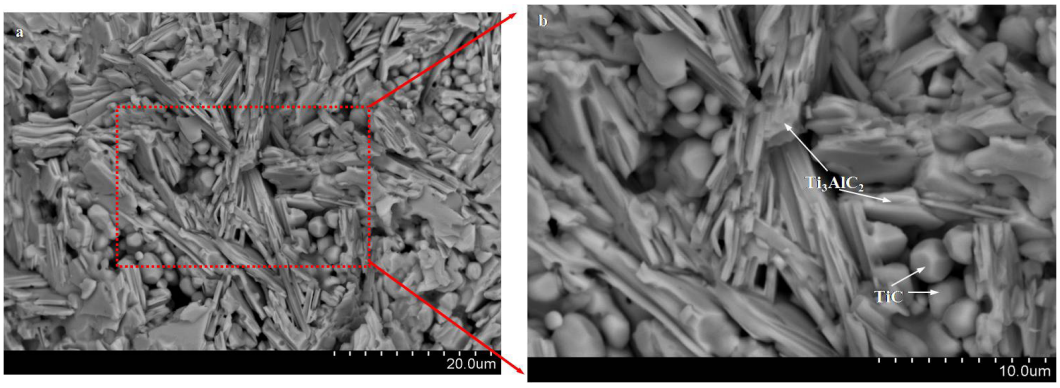

Fig. 12. Fracture microstructure of the material synthesized from MA raw mixture using force SHS-pressing. Magnification ×2000 (a), ×4000 (b).

3. The effect of MA on the character and kinetics of combustion front propagation has been investigated. As a result of mechanical activation, the combustion mode changes from stationary to pulsating and, consequently, the combustion rate decreases. When the duration of MA is from 1 to 3 min, the combustion rate increases due to the accumulation of energy at the structure defects and enhancement of the reactant specific surface area during the formation of composite granules with a layered structure. When the duration of MA is increased to 4 min, the combustion rate decreases again.

4. Due to MA, the compacted products synthesized by force SHS-pressing have a homogeneous structure and higher content of Ti_3AlC_2 MAX phase.

Acknowledgements

The authors gratefully acknowledge the financial support from the Russian Scientific Foundation (Agreement No. 14-19-00273).

References

[1]. N.V. Tzenov, M.W. Barsoum. J. Am. Ceram. Soc. 83 (2000) 825–832.
[2]. Chunfeng Hu, Haibin Zhang, Fangzhi Li, Qing Huang, Yiwang Bao. Int. J. Refract. Met. Hard Mater. 36 (2013) 300–312.
[3]. E.A. Levashov, Yu.S. Pogozhev, D.V. Shtansky, M.I. Petrzhik. Russian Journal of Non-Ferrous Metals 50 (2009) 151–160.
[4]. W.K. Pang, I.M. Low, Understanding and improving the thermal stability of layered ternary carbides in ceramic matrix composites in book Advances in Ceramic Matrix Composites: I.M. Low (Eds.), Woodhead Publishing Limited, Philadelphia, USA, 2014, pp. 340–368.
[5]. C.B. Spencer, Fiber-Reinforced Ti_3SiC_2 and Ti_2AlC MAX Phase Composites. A Thesis of Master of Science in Materials Science and Engineering. Drexel University. 2010. 92 p.
[6]. X.H. Wang, Y.C. Zhou, J. Mater. Sci. Technol. 26 (2010) 385–416.
[7]. M.A. Pietzka, J.C. Schuster. J. Phase Equilib. 15 (1994) 392–400.
[8]. M.W. Barsoum, D. Brodkin, T. El-Raghy. Scripta Materialia 36 (1997) 535–541.
[9]. Y. Khoptiar, I. Gotman, E.Y. Gutmanas. J. Am. Ceram. Soc. 88 (2005) 28–33.
[10]. Aiguo Zhou, Chang-An Wang, Zhenbin Ge, Lifeng Wu. J. Mater. Sci. Lett. 20 (2001) 1971–1973.
[11]. Shinobu Hashimoto, Masaru Takeuchi, Koji Inoue, Sawao Honda, Hideo Awaji, Koichiro Fukuda, Shaowei Zhang. Mater. Lett. 62 (2008) 1480–1483.
[12]. W.B. Zhou, B.C. Mei, J.Q. Zhu, X.L. Hong. Mater. Lett. 59 (2005) 131–134.
[13]. M.W. Barsoum, M. Ali, T. El-Raghy. Metall. Mater. Trans. A 31 (2000) 1857–1865.
[14]. Zhenbin Ge, Kexin Chen, Junming Guo, Heping Zhou, José M. F. Ferreira. J. Eur. Ceram. Soc. 23 (2003) 567–574.
[15]. Shinobu Hashimoto, Noriko Nishina, Kiyoshi Hirao, You Zhou, Hideki Hyuga, Sawao Honda, Yuji Iwamoto. Mater. Res. Bull. 47 (2012) 1164–1168.
[16]. A.F. Fedotov, A.P. Amosov, E.I. Latuhin, A.A. Ermoshkin, D.M. Davydov. Izvestija Samarskogo nauchnogo centra Rossijskoj akademii nauk [Proceedings of the Samara Scientific Center of the Russian Academy of Sciences] 16 (2014) 50–55 (in Russian).
[17]. D.V. Shtansky, F.V. Kiryukhantsev-Korneev, A.N. Sheveyko, B.N. Mavrin, E.A. Levashov, C. Rojas, A. Fernandez. Surf. Coat. Technol. 203 (2009) 3595–3609.

[18]. E.A. Levashov, A.E. Kudryashov, Yu.S. Pogozhev, P.V. Vakaev, E.I. Zamulaeva, T.A. Sviridova. Russian Journal of Non-Ferrous Metals 48 (2007) 362–372.
[19]. M. Yoshida, Ya. Hoshiyama, J. Ommyoji, A. Yamaguchi. Mater. Sci. Eng., B 173 (2010) 126–129.
[20]. Shi-Bo Li, Hong-Xiang Zhai, Guo-Ping Bei, Yang Zhou, Zhi-Li Zhang. Ceram. Int. 33 (2007) 169–173.
[21]. A. Hendaoui, M. Andasmas, A. Amara, A. Benaldjia, P. Langlois, D. Vrel. International Journal of Self-Propagating High-Temperature Synthesis 17 (2008) 129–135.
[22]. A. Hendaoui, D. Vrel, A. Amara, P. Langlois, M. Andasmas, M. Guerioune. J. Eur. Ceram. Soc. 30 (2010) 1049–1057.
[23]. D.P. Riley, E.H. Kisi, D. Phelan. J. Eur. Ceram. Soc. 26 (2006) 1051–1058.
[24]. E.A. Levashov, V.V. Kurbatkina, E.I. Patsera, Yu.S. Pogozhev, S.I. Rupasov, A.S. Rogachev. Russian Journal of Non-Ferrous Metals 51 (2010) 403–433.
[25]. K.N. Egorychev, V.V. Kurbatkina, E.A. Levashov. Izvestija VUZov. Cvetnaja metallurgija [Proceedings of the universities. Non-ferrous metallurgy] 6 (1996) 49–52 (in Russian).
[26]. V.V. Kurbatkina, E.A. Levashov, Mechano-activation of SHS in book combustion of heterogeneous systems: fundamentals and applications for materials synthesis, in: A.S. Mukasyan, K.S. Martirosyan (Eds.), Trans-world Research Network, Kerala, India, 2007, pp. 131–141.
[27]. N.Z. Lyakhov, T.L. Talako, T.F. Grigorieva: Effect of mechanical activation on the processes of phase- and structure formation during self-propagating high-temperature synthesis. Novosibirsk: Parallel, 2008 (in Russian).
[28]. V. Gauthier, C. Josse, F. Bernard, E. Gaffet, J.P. Larpin. Mater. Sci. Eng., A 265 (1999) 117–128.
[29]. V. Gauthier, F. Bernard, E. Gaffet, C. Josse, J.P. Larpin. Mater. Sci. Eng., A 272 (1999) 334–341.
[30]. L.L. Ye, M.X. Quan. Nanostruct. Mater. 5 (1995) 25–31.
[31]. I. Radja, H. Djelad, E. Morallon, A. Benyoucef. Synth. Met.202 (2015) 25–32.
[32]. E.A. Levashov, V.V. Kurbatkina, K.V. Kolesnichenko. Izvestija VUZov. Cvetnaja metallurgija [Proceedings of the universities. Non-ferrous metallurgy] 6 (2000) 61–67 (in Russian).
[33]. F. Maglia, U. Anselmi-Tamburini, G. Cocco, M. Monagheddu, N. Bertolino, Z.A. Munir. J. Mater. Res. 16 (2001) 1074–1082.
[34]. A.S. Rogachev, J.-C. Gachon, H.E. Grigoryan, D. Vrel, J.C. Schuster, N.V. Sachkova. Journal of materials science 40 (2005) 2689–2691.
[35]. V.K. Smolyakov. Combustion of Mechanically Activated Heterogeneous Systems. Combustion, Explosion and Shock Waves 41 (2005) 319–325.
[36]. L.V. Zueva, A.I. Gusev. Phys. Solid State. 41 (1999) 1032–1038.